KNOTS AND PARTICLES

L. Faddeev[*♯] **and Antti J. Niemi**[**♯]

[*] *St.Petersburg Branch of Steklov Mathematical Institute*
Russian Academy of Sciences, Fontanka 27 , St.Petersburg, Russia[‡]

[**] *Department of Theoretical Physics, Uppsala University*
P.O. Box 803, S-75108, Uppsala, Sweden[‡]

and

[♯] *Research Institute for Theoretical Physics*
P.O. Box 9, FIN-00014 University of Helsinki, Finland

Using methods of high performance computing, we have found indications that knotlike structures appear as stable finite energy solitons in a realistic 3+1 dimensional model. We have explicitly simulated the unknot and trefoil configurations, and our results suggest that all torus knots appear as solitons. Our observations open new theoretical possibilities in scenarios where stringlike structures appear, including physics of fundamental interactions and early universe cosmology. In nematic liquid crystals and ^{3}He superfluids such knotted solitons might actually be observed.

[‡] permanent address

[*] supported by Russian Academy of Sciences and the Academy of Finland

[**] Supported by Göran Gustafsson Foundation for Science and Medicine and by NFR Grant F-AA/FU 06821-308

[*] E-mail: **FADDEEV@PDMI.RAS.RU and FADDEEV@PHCU.HELSINKI.FI**

[**] E-mail: **ANTTI.NIEMI@TEORFYS.UU.SE**

In 1867 Lord Kelvin [1] proposed that atoms, which at the time were considered as elementary particles, are knotted vortex tubes in ether. For about 20 years his theory was taken seriously, and motivated an extensive study of knots. The results obtained at the time by Tait [2] remain a classic contribution to mathematical knot theory [3]. More recently the idea that elementary particles can be identified with topologically distinct knots has been advanced in particular by Jehle [4].

Today it is commonly accepted that fundamental interactions are described by string-like structures [5], with different elementary particles corresponding to the vibrational excitations of a fundamental string. Even though there are hints of connections between modern string theory and knot theory [6], knotlike structures have not yet been of much significance.

There are also a number of other scenarios where knotted structures may enter Physics [3], [7]. These include models in statistical physics, QCD strings that confine quarks inside nuclear particles, cosmic strings that are expected to be responsible for early universe structure formation, and approaches to quantum gravity where knots are supposed to determine gauge invariant observables. Stringlike vortices appear in type-II superconductors where they confine magnetic fields within the cores of vortex-like structures, and similar phenomena are also present in superfluid ^{4}He. Recent experiments with nematic liquid crystals [8] and ^{3}He superfluids [9] have also revealed interesting vortex structures that can be described by theoretical methods which are adopted from cosmic string models. Finally, physics of knots is rapidly becoming an important part of molecular biology, where entanglement of a DNA chain interferes with vital life processes of replication, transcription and recombination [10].

Thus far the physics of knotlike structures has been investigated sparsely. This is largely due to a lack of dynamical principles that enable the construction of stable knots. One needs a theoretical model where knots emerge as solitons, *i.e.* as stable finite energy solutions to the pertinent nonlinear field equations.

The literature on solitons is enormous, and there are several extensive reviews [7], [11], [12]. Until now the activity has mainly concentrated on 1+1 dimensions with the notable exceptions of the 2+1 dimensional vortex and nonlinear σ-model soliton, and skyrmeons and 'tHooft-Polyakov monopoles in 3+1 dimensions. These are all pointlike configurations, and can not be directly associated with knotlike structures.

When embedded in three dimensions, a pointlike two dimensional soliton becomes a line vortex. For a finite energy its length must be finite which is possible if its core forms a knot. In 1975 one of us [13] proposed that closed, knotted vortices could be constructed in a definite dynamical model. The explicit solution suggested in [13] is a closed torus-like vortex ring, twisted once around its core before joining the ends which ensures stability against shrinking. This closed vortex corresponds to the *unknot* (see figure 4) which is the simplest possible knotlike structure. However, despite numerous attempts no such stable configuration has been constructed, neither by explicit analysis nor by a numerical investigation.

Here we shall report on our work to construct knotlike vortices in the model introduced in [13]. By employing numerical algorithms in powerful computers we have been able to find strong evidence for the existence of the unknot vortex. In addition we have found indications supporting the existence of a *trefoil* vortex (see figure 5). A trefoil is the simplest example of torus-knots, which are obtained by winding around a torus in both directions [3]. Our results suggest that in fact all torus knots should appear as vortex solitons in the model proposed in [13]. This model describes the 3+1 dimensional dynamics of a three component vector $\vec{\mathbf{n}}(\mathbf{x},\tau)$ with unit length, $\vec{\mathbf{n}}\cdot\vec{\mathbf{n}}=1$. Such a vector field is a typical degree of freedom in the nonlinear σ-model, a prototype relativistic quantum field theory. It also appears as an order parameter in the Heisenberg ferromagnet. A unit vector field is also present in models of nematic liquid crystal where it characterizes the average direction of the rod, and in ^{3}He-A superfluid where it determines the spin projection direction for a Cooper pair. Indeed, the model proposed in [13] is quite universal, and we expect our results to have a large number of applications.

In order that $\vec{\mathbf{n}}(\vec{\mathbf{x}})$ describes a localized stationary knot, it must go to a constant vector $\vec{\mathbf{n}}(\vec{\mathbf{x}})\rightarrow\vec{\mathbf{n}}_0$ at large distances. Consequently $\vec{\mathbf{n}}(\vec{\mathbf{x}})$ defines a mapping from the compactified $R^3\sim S^3\rightarrow S^2$. Such mappings fall into nontrivial homotopy classes $\pi_3(S^2)\simeq Z$ and can be characterized by the Hopf invariant [3]. For this we introduce the two-form $F=(d\vec{\mathbf{n}}\wedge d\vec{\mathbf{n}},\vec{\mathbf{n}})$ on the target S^2. Its preimage $F_\star$ on S^3 is exact, $F_\star=dA_\star$, and the Hopf invariant Q_H is given by

$$Q_H \;=\; \int\limits_{R^3} F\wedge A \tag{1}$$

The Hamiltonian proposed in [13] is

$$H \;=\; E_2 \;+E_4 \;=\; \int d^3x\; g^2(\partial_\mu\vec{\mathbf{n}})^2+e^2F^2 \tag{2}$$

This is the most general three dimensional Hamiltonian that admits a relativistically invariant extension in 3+1 dimensions and involves only terms with no more than four derivatives. It can be related to the $SU(2)$ Skyrme model when restricted to a sphere $S^2\in SU(2)$, but its topological features are different. In particular, the existence of nontrivial knotted vortex solutions in (2) is strongly suggested by the lower bound $H\geq c\cdot|Q_H|^{\frac{3}{4}}$ [14].

The first term E_2 determines the standard nonlinear O(3) σ-model which admits static solitons in two dimensions. But in three dimensions a scaling $\vec{\mathbf{x}}\rightarrow\rho\vec{\mathbf{x}}$ reveals that stable stationary solutions are possible only if E_4 is also present. Indeed, under this scaling $E_2\rightarrow\rho E_2$ but $E_4\rightarrow\rho^{-1}E_4$ from which we conclude that in three dimensions finite energy solutions obey the virial theorem,

$$E_2 \;=\; E_4 \tag{3}$$

Several articles have been devoted for analyzing the general properties of the unknot vortex in the model (2) [12]. However, to our knowledge there have been no real attempts to find an actual solution. This is due to the fact, that even in the simplest case of an unknot the separation of variables eliminates only one of the three space coordinates, leaving numerical methods as the sole alternative for finding a solution. With the recent, enormous progress in supercomputing techniques serious attempts are finally becoming realistic.

The Euler-Lagrange equations for (2) determine a highly nonlinear elliptic system, and a direct numerical approach appears to be complicated. Instead, we consider the parabolic equation

$$\frac{d\phi_a}{dt} \;=\; -\,\frac{\delta H(\phi)}{\delta \phi_a} \tag{4}$$

where ϕ_a denotes a generic dynamical variable in (2). The t-bounded solutions of (4) connect the critical points of H by flowing away from an unstable critical point at $t \to -\infty$ towards a stable critical point at $t \to +\infty$. From this we expect that by defining a suitable initial configuration at $t = 0$, for large $t \gg 0$ we flow towards a stable vortex solution of the original stationary equation.

We parametrize our unit vector by $\vec{\mathbf{n}} = (\cos\varphi \sin\theta, \sin\varphi \sin\theta, \cos\theta)$ through stereographic coordinates $\varphi = -\arctan(\frac{V}{U})$ and $\theta = 2\arctan\sqrt{U^2+V^2}$. In terms of these variables the Hamiltonian (2) becomes

$$H = \int d^3x \; \frac{4g^2}{(1+U^2+V^2)^2}(\partial_\mu U^2 + \partial_\mu V^2) + \frac{16e^2}{(1+U^2+V^2)^4}(\partial_\mu U \partial_\nu V \;-\; \partial_\nu U \partial_\mu V)^2 \tag{5}$$

By a global $SO(3)$ rotation we can select our asymptotic vacuum vector $\vec{\mathbf{n}}_0$ so that outside of the vortex it points to the positive-z direction. This means that outside of the vortex we are near the north pole where $\theta(\vec{\mathbf{x}}) \approx 0$, while the core corresponds to the south pole $\theta(\vec{\mathbf{x}}_c) = \pi$. The internal structure of a vortex can then be investigated by cutting it once with a plane at right angle to its core. This cross sectional plane is topologically identical to a sphere S^2: At the core we have $\theta(\vec{\mathbf{x}}_c) = \pi$ corresponding to the south pole and outside of the vortex on the plane we have $\theta(\vec{\mathbf{x}}) \approx 0$ corresponding to the north pole. Furthermore, $\varphi(\vec{\mathbf{x}})$ increases (or decreases, depending on orientation) by 2π when we go around the core once on the cross sectional plane.[1] For $U$and V this means, that we identify them as local coordinates on the Riemann sphere in a patch that contains the north pole $U(\vec{\mathbf{x}}) = V(\vec{\mathbf{x}}) = 0$.

In figures 1 and 2 we have drawn $\theta(\vec{\mathbf{x}})$ and $\varphi(\vec{\mathbf{x}})$ respectively for our unknot vortex. The general structure is clearly visible in these pictures.

In the present model there are two symmetries that relate a given vortex solution with Hopf invariant Q_H to an antivortex solution with equal energy but opposite Hopf

[1] More generally, φ is defined modulo $2\pi n$ where n is an integer. Here we only consider the simplest case with $n = \pm 1$.

invariant $-Q_H$. The first symmetry emerges when we change orientation $\varphi \to -\varphi$ on the cross sectional plane. The second symmetry interchanges the north pole with the south pole on the cross sectional plane, *i.e.* maps the core to $\theta(\vec{\mathbf{x}}_c) = 0$ and the region outside of the vortex to $\theta(\vec{\mathbf{x}}) \approx \pi$. In terms of the $U(\vec{\mathbf{x}})$ and $V(\vec{\mathbf{x}})$ variables this means that on each cross sectional plane the Hamiltonian (5) must be invariant under the inversion $Z(\vec{\mathbf{x}}) = U(\vec{\mathbf{x}}) + iV(\vec{\mathbf{x}}) \to Z^{-1}(\vec{\mathbf{x}})$. This implies in particular, that the energy density $H(\vec{\mathbf{x}})$ must be concentrated in a relatively narrow tubular neighborhood around the core of the vortex.

In figure 3 we have depicted the energy density on a cross sectional plane for the unknot vortex. The concentration of energy density in a tubular manner around the core is clearly visible.

In order to specify the initial condition in (4) we need a knot configuration which is topologically equivalent to the desired vortex solution. We specify this configuration by first introducing a parametrization $\vec{\mathbf{x}}(\lambda)$ for the center of the knot in R^3, and then for each λ use the Serret-Frenet equations to define local coordinates $U(\vec{\mathbf{x}}; \lambda)$ and $V(\vec{\mathbf{x}}; \lambda)$ on the cross sectional planes.

The choice of initial parametrization $\vec{\mathbf{x}}(\lambda)$ for the core introduces a scale which may be quite different from the one specified by the coupling constant g in (5). In order to enhance convergence, we adopt a simple renormalization procedure by promoting g to a time dependent function $g(t)$. We define this time dependence by demanding that at each value of t the virial theorem (3) must be obeyed. Since a vortex solution obeys (3), this means that $g(t)$ flows towards a fixed point value $g(t) \ \to \ g^\star$.

We have performed our numerical simulations using version 5.3 of G. Sewell's PDE2D finite element algorithm [15]. During the early phase of our simulations we have used the initial knot configuration to determine the boundary conditions on the finite element mesh. However, since the exact boundary conditions for the desired vortex are *a priori* unknown, after several time steps we have decreased the size of the finite element mesh and used the pertinent simulated configuration to determine the boundary conditions in the new mesh. By starting from a sufficiently large initial mesh, we then eventually obtain a submesh with boundary conditions that are close to those of the actual solution.

For our simulation we have used two Silicon Graphics Power Challenge computers with R8000 processors equipped with 1GB *resp.* 2GB of internal memory.

For the unknot vortex ($Q_H = \pm 1$), the equations of motion can be simplified using axial symmetry. We select the symmetry axis to coincide with the z-axis in R^3, and introduce cylindrical coordinates r, ϕ, z. With the Ansatz $\varphi(\vec{\mathbf{x}}) = \varphi(r, z) + \phi$ and $\theta(\vec{\mathbf{x}}) = \theta(r, z)$ the ϕ-coordinate separates, and we obtain a two dimensional equation for $U(r, z)$ and $V(r, z)$. That such a separation of variables is possible follows directly from the $SO(2) \times SO(2)$ symmetry of the unknot configuration. The ensuing equations are defined on the half-plane $r \geq 0$, $z \in (-\infty, \infty)$, which at each ϕ determines our cross sectional

plane. Besides the inversion invariance, the equations of motion are now also invariant under $z \to -z$. Since the unknot solution is even in z, this halves the CPU time in our simulation.

In figures 1-4 we describe an unknot vortex which is a result of over 50h of CPU time with each time step taking about 9 minutes on a 9600 triangle mesh. The mesh has been selected so that it is more dense at the boundaries and near the core of the vortex. In our simulation we find impressive convergence, allowing us to increase the time step by up to 8 orders of magnitude while keeping the relative change in energy intact. The Hopf invariant is also very stable, and we have identified the final configuration on the basis that the numerically computed Hopf invariant has a slight local maximum with $Q_H = 0.999996$ ...

The trefoil vortex ($Q_H = \pm 3$) described in figure 5 is a result of almost 200h in CPU time on a 21^3 cubic finite element lattice with tri-cubic Hermite basis functions. Consequently the number of nodes is about the same as in the case of unknot, but due to a lack of any obvious reflection symmetry each time iteration now takes about 20 minutes of CPU time. The yellow center in figure 5 corresponds to the core $\vec{\mathbf{x}}(\lambda)$ of our initial configuration, which has been determined using the energy concept developed by J. Simon [16]. The points in figure 5 have been evaluated using the piecewise cubic polynomial approximation obtained from the finite element algorithm. As in figure 4, the picture describes a volume where the energy density inside the vortex essentially vanishes, *i.e.* it can be viewed as an extended core of our trefoil vortex.

We expect that the nonhomogeneity in figure 5 reflects the underlying lattice structure that we have used in our simulation. Indeed, a 21^3 lattice is obviously too rough to describe our trefoil solution adequately, but unfortunately we do not have access to a computer that would allow us to use an essentially larger lattice. Nevertheless, we have found definite numerical stability in the sense that the final configuration in figure 5 has remained essentially intact under a large number of iterations. We view this stability as a strong evidence that we indeed have convergence towards a trefoil vortex solution.

In conclusion, we have performed numerical simulations with a high-performance computer to investigate knotted vortex solutions in the model introduced in [13]. By investigating the unknot and trefoil vortices, we have found strong evidence that torus knots indeed appear as solitons. For the unknot, we have found very impressive convergence and our results for the trefoil are also quite encouraging. However, since the computers we can access do not allow us to effectively study dense three dimensional lattices, our simulation of the trefoil is still tentative.

We expect that our results will have numerous important applications. In particular, since the order parameter in nematic liquid crystal and ^{3}He superfluid involves a unit three vector, an experimental investigation of vortices in these materials should reveal the existence of stable knotlike structures. We also expect that an extension of our work

to spontaneously broken Yang-Mills-Higgs theories where stable knotlike vortices can not be excluded by scaling arguments, should have interesting physical implications in particular to early universe cosmology.

We wish to thank J.Hietarinta, T.Kärki, A.P.Niemi, K.Palo, J.Pitkäranta, J.Rahola, D.Riska, R.Scharein, G.Sewell, O.Tirkkonen and J.Tulkki for helpful discussions and valuable suggestions. We are particularly indebted to Sami Virtanen for his help with visualization and simulating the initial Ansatz for the trefoil, and Matti Gröhn for helping us with visualization. We are grateful to the Center for Scientific Computing in Espoo, Finland for providing us with an access to their line of Silicon Graphics Power Challenge computers.

References

[1] W.H. Thomson, Trans. R. Soc. Edin. **25** (1869) 217

[2] P.G. Tait, *On Knots I, II, III* Scientific Papers, Cambridge University Press, 1990

[3] M. Atiyah, *The geometry and physics of knots*, Cambridge University Press, 1990; L.H. Kauffman, *Knots and physics*, World Scientific, 1993

[4] H. Jehle, Phys. Rev. **D6** (1972) 441

[5] M.B. Green, J.H. Schwarz and E. Witten, *Superstring theory I, II* Cambridge University Press, 1987

[6] E. Witten, Commun. Math. Phys. *121* (1989) 351

[7] C. Rebbi and G. Soliani, *Solitons and Particles* World Scientific, 1984

[8] M.J. Bowick, L. Chander, E.A. Schiff and A.M. Srivastava, Science **263** (1994) 943

[9] C. Bäuerle *et. al.*, Nature **382** (1996) 332; V.M.H. Ruutu *et. al.*, Nature **382** (1996) 334

[10] D.W. Sumners, Notices of AMS **42** (1995) 528

[11] L.D. Faddeev and L.A. Takhtajan, *Hamiltonian methods in the theory of solitons*, Springer-Verlag, 1987

[12] V.D. Makhankov Y.P. Rybakov and V.I. Sanyuk, *The Skyrme model: fundamentals, methods, applications* Springer-Verlag, 1993

[13] L. Faddeev, *Quantisation of solitons*, preprint IAS Print-75-QS70 ,1975; and in *Einstein and several contemporary tendencies in the field theory of elementary particles* in Relativity, quanta and cosmology vol. 1, M. Pantaleo and F. De Finis (eds.), Johnson Reprint, 1979

[14] A.F. Vakulenko and L.V. Kapitanski, Dokl. Akad. Nauk USSR *248* (1979) 810

[15] G. Sewell, Adv. Eng. Software **17** (1993) 105

[16] J.K. Simon, Journ. Knot Thy. and Raminif. **3** (1994) 299

Figure Caption

Figure 1: A combined surface and contour plot of $\theta(r, z)$ for an unknot vortex with $g^\star \approx 0.24,\ e = 1$ in cylindrical coordinates (r, ϕ, z) and on a cross sectional plane with generic ϕ. The configuration is $z \to -z$ symmetric.

Figure 2: A combined surface and contour plot of $\varphi(r, z)$ for the unknot vortex. The line where φ jumps by π is clearly visible. The configuration is $z \to -z$ symmetric.

Figure 3: A combined surface and contour plot of energy density $H(r, z)$ for the unknot vortex, for comparison as figure 1. The configuration is $z \to -z$ symmetric.

Figure 4: Three dimensional view of the extended core for the unknot vortex. The core is defined as the region where energy density essentially vanishes.

Figure 5: The same as figure 5 but for a trefoil with $g^\star \approx 1.3,\ e = 1$. The center denotes the core of the initial configuration, determined using a minimum energy principle [16]. We thank J. Simon for providing us with the initial parametrization.

figure 2

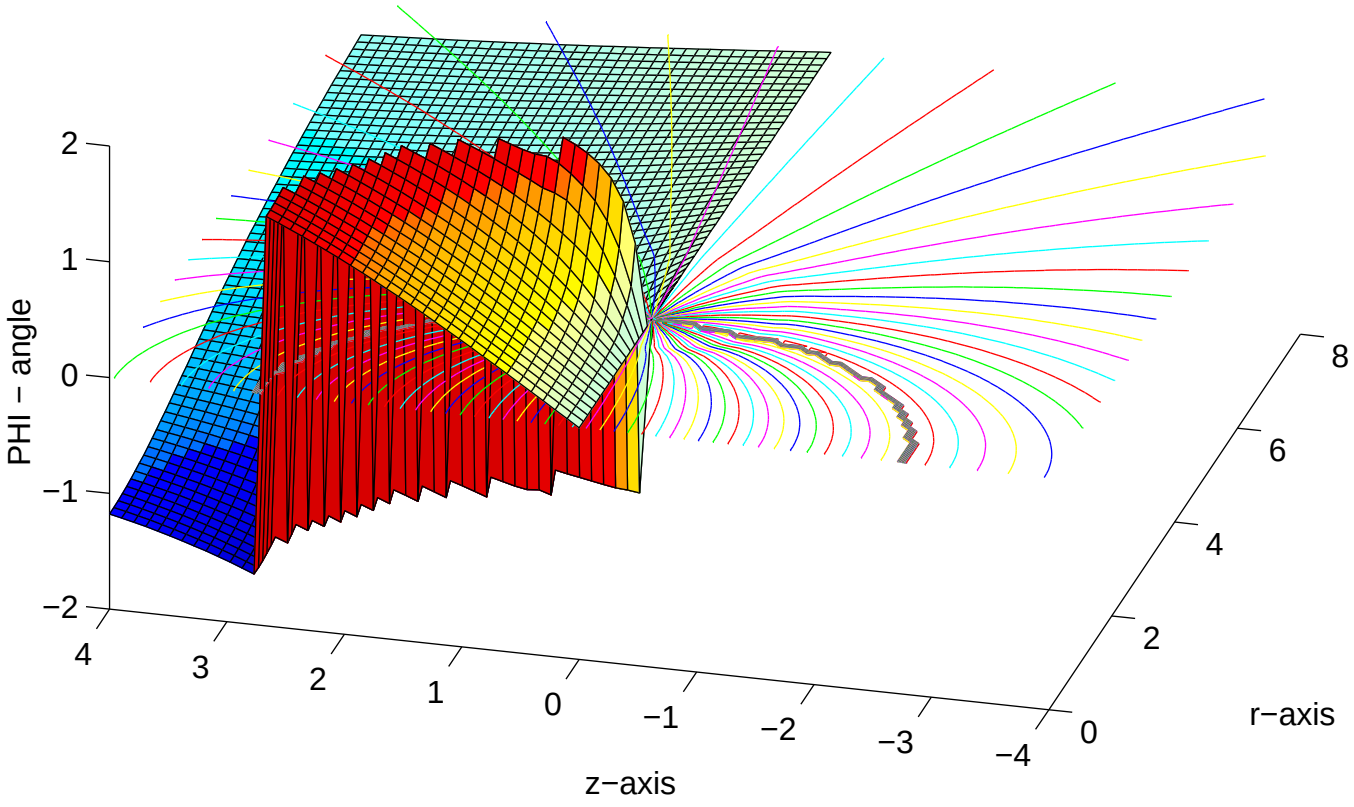

figure 3

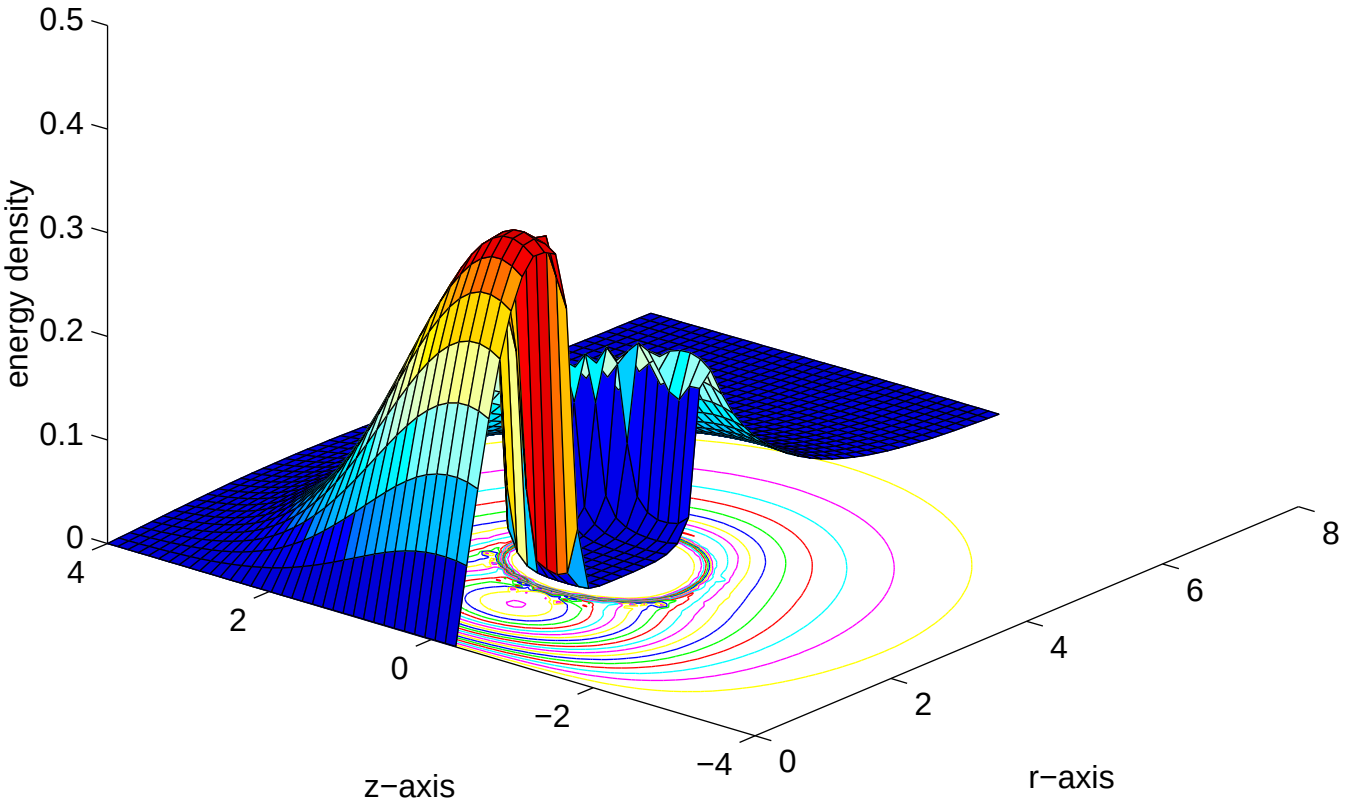

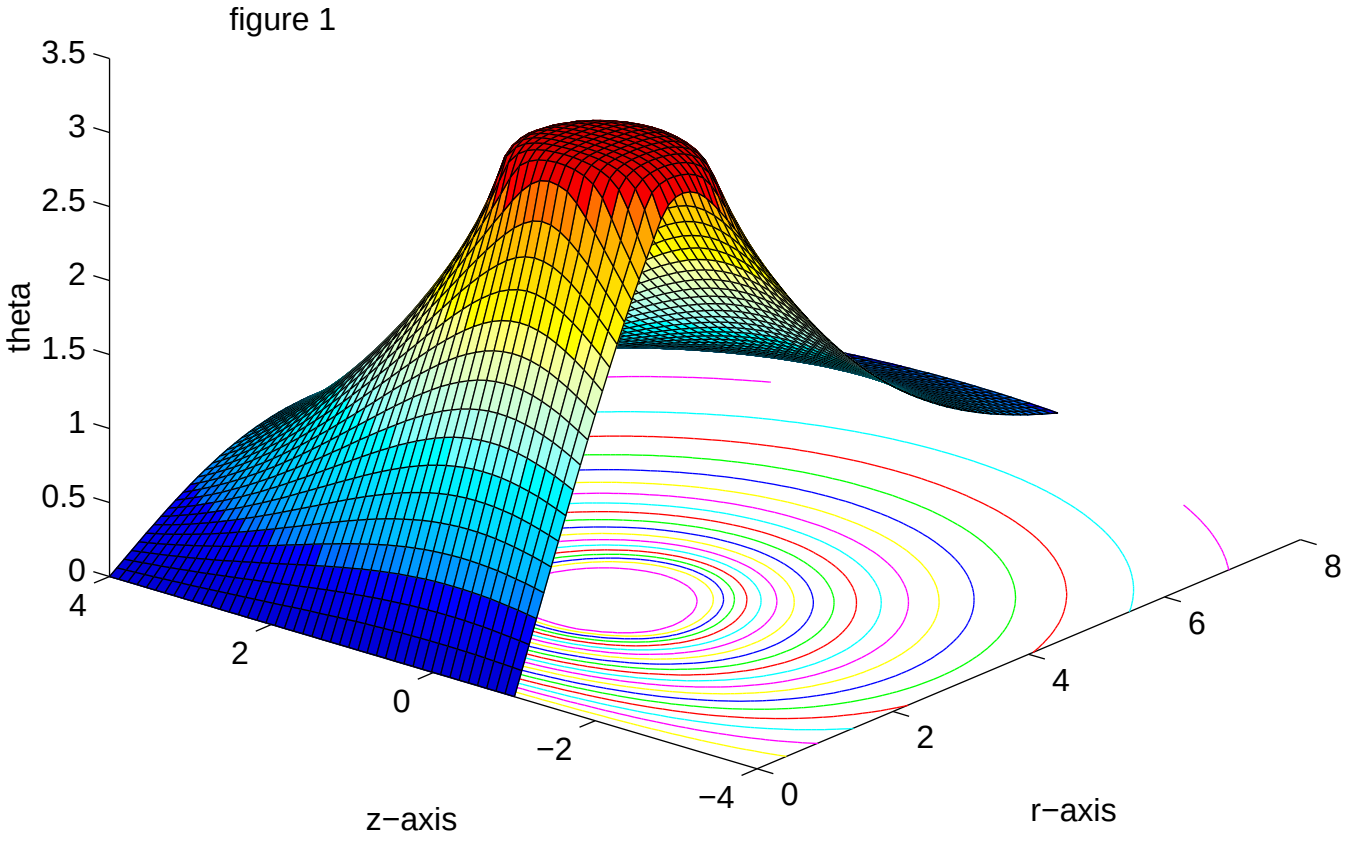
figure 1
theta
3.5
3
2.5
2
1.5
1
0.5
0
4
2
0
−2
−4
z−axis
0
2
4
6
8
r−axis

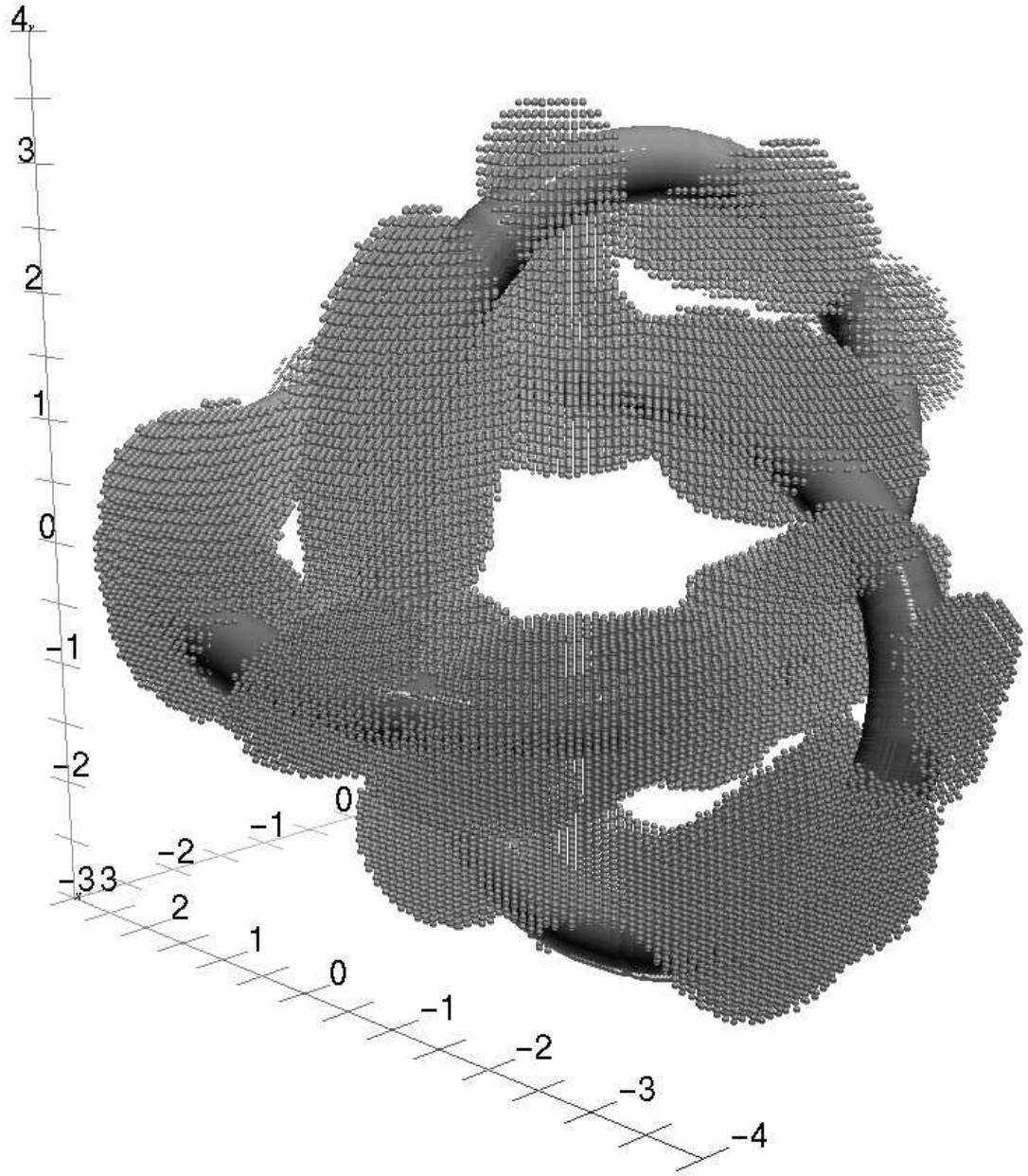
4
3
2
1
0
−1
−2
−3
3
2
1
0
−1
−2
−3
−4

figure 4